View metadata, citation and similar papers at core.ac.uk
brought to you by CORE
provided by KITopen

Research article

Aso Rahimzadegan*, Dennis Arslan, David Dams, Achim Groner, Xavi Garcia-Santiago, Rasoul Alaee, Ivan Fernandez-Corbaton, Thomas Pertsch, Isabelle Staude and Carsten Rockstuhl

Beyond dipolar Huygens' metasurfaces for full-phase coverage and unity transmittance

https://doi.org/10.1515/nanoph-2019-0239
Received September 6, 2019; revised October 24, 2019; accepted November 14, 2019

Abstract: Metasurfaces made from densely packed resonant wavelength-scale particles enable abrupt modulation of impinging electromagnetic radiation within an ultrathin surface. Combining duality symmetry of particles and rotational symmetry of their arrangement led to the development of Huygens' metasurfaces with perfect transmission. However, so far, when identical particles are considered, only their dipolar multipolar contributions are engineered. There, the achievable phase coverage at a fixed wavelength when modifying the period is smaller than 2π, being a clear limitation for applications. To lift such limitation, we consider dipolar-quadrupolar Huygens' metasurfaces. They consist of scatterers that require a dipolar and a quadrupolar term to capture their response. We show that such metasurfaces offer access to the desired 2π phase coverage while preserving the perfect efficiency when the conditions of duality and symmetry continue to be met. We also propose core-multishell and disk-multiring particles made from realistic materials to meet the requirements and that can be used to build such metasurfaces. Our results are important as a theoretical basis for large-scale fabrications in imaging and integrated optics.

Keywords: Huygens' metasurface; multipoles expansion method; scattering theory; hologram; duality symmetry.

PACS: 42.25.-p; 42.70.-a; 78.67.Bf; 76.60.Gv.

***Corresponding author: Aso Rahimzadegan,** Institute of Theoretical Solid State Physics, Karlsruhe School of Optics and Photonics, Karlsruhe Institute of Technology, Wolfgang-Gaede-Str. 1, D-76131 Karlsruhe, Germany, e-mail: aso.rahimzadegan@kit.edu. https://orcid.org/0000-0002-9467-2937
Dennis Arslan: Institute of Applied Physics, Abbe Center of Photonics, Friedrich Schiller University Jena, 07745 Jena, Germany
David Dams, Achim Groner and Xavi Garcia-Santiago: Institute of Theoretical Solid State Physics, Karlsruhe Institute of Technology, Wolfgang-Gaede-Str. 1, D-76131 Karlsruhe, Germany
Rasoul Alaee: Max Planck Institute for the Science of Light, 91058 Erlangen, Germany; and Department of Physics, University of Ottawa, Ottawa, ON K1N 6N5, Canada
Ivan Fernandez-Corbaton: Institute of Nanotechnology, Karlsruhe Institute of Technology, 76021 Karlsruhe, Germany
Thomas Pertsch: Institute of Applied Physics, Abbe Center of Photonics, Friedrich Schiller University Jena, 07745 Jena, Germany; and Fraunhofer Institute for Applied Optics and Precision Engineering, Albert-Einstein-Str. 7, 07745 Jena, Germany. https://orcid.org/0000-0003-4889-0869
Isabelle Staude: Institute of Applied Physics, Abbe Center of Photonics, Friedrich Schiller University Jena, 07745 Jena, Germany. https://orcid.org/0000-0001-8021-572X
Carsten Rockstuhl: Institute of Theoretical Solid State Physics, Karlsruhe Institute of Technology, Wolfgang-Gaede-Str. 1, D-76131 Karlsruhe, Germany; and Institute of Nanotechnology, Karlsruhe Institute of Technology, 76021 Karlsruhe, Germany, https://orcid.org/0000-0002-5868-0526

1 Introduction

Huygens' metasurfaces, i.e. metasurfaces made from an n-fold rotationally symmetric $C_{n>2}$ arrangement of resonant scatterers that are electromagnetically dual-symmetric [1], are characterised by a suppressed back-reflection [2]. Made out of nonabsorbing particles, these metasurfaces provide unity optical transmittance while allowing to tune the phase angle of the transmission [3–8]. Huygens' metasurfaces are appealing candidates to implement wavefront modulation devices such as holograms in ultrathin surfaces [9]. In Huygens' metasurfaces, the excited electric and magnetic moments of the scatterers have to be equal. Thus far, emphasis had been put on dipolar metasurfaces, i.e. metasurfaces where the scattering response from its constituents can be explained while considering only the dipolar contribution [4, 10–12]. This corresponds to the idea of a Huygens' source that lent the device its name.

For a fixed geometry and by sweeping through the resonance in frequency domain, the phase angle of transmission through Huygens' metasurfaces can be tuned to

Open Access. © 2019 Aso Rahimzadegan et al., published by De Gruyter. This work is licensed under the Creative Commons Attribution 4.0 Public License.

Bereitgestellt von | Karlsruher Institut für Technologie KIT-Bibliothek
Angemeldet
Heruntergeladen am | 27.01.20 13:02

cover the entire 2π range [4]. However, the metasurfaces are not operated at various but at a fixed frequency. Therefore, the phase angle of the transmission should be tuned by either locally tuning the geometry of the particles for a fixed arrangement or tailoring the arrangement of otherwise identical particles. At a fixed operational frequency, enforcing an equal electric and magnetic response requires a careful design of the geometry of the particle.

Our study is focused on metasurfaces with identical particles. For large-scale self-assembled metasurfaces, having identical particles is highly demanding. Due to fabrication constraints, the consideration of multiple particles satisfying the required conditions such as unity transmittance and a desired transmission phase angle is daunting. For example, designing Huygens' metasurfaces with nanocylinders having equal electric and magnetic response under normal incidence requires a specific aspect ratio of radius over height but different absolute sizes for different transmission phase angles. This implies that different heights across the (meta)surface are required for a unity transmittance and full-phase coverage. Such a requirement is clearly not suited for lithography. Therefore, as an additional constraint, we shall require the metasurface to be made from identical particles. And the only tuning parameter that is left over in such configuration is the lattice constant that tunes the arrangement of the particles.

However, as we will demonstrate shortly, by sweeping through the lattice constant and while considering only dipolar particles, it is nearly impossible to cover the entire 2π range of transmission phase angles at a fixed operational wavelength. To entirely lift such limitation, we propose here to exploit quadrupolar resonances in the scatterers along with the dipolar resonances to access the entire phase-shift range of 2π.

It is worth noting here that high-transmittance nonresonant and non-Huygens' metasurfaces that can provide the full-phase coverage are possible. In these metasurfaces, nonidentical particles can be used [10, 13–17]. In this contribution, our focus is on resonant polarisation-insensitive Huygens' metasurfaces made out of identical rotational-symmetric particles.

To analyse in this contribution the transmission through dielectric metasurfaces in a generic and systematic approach, we initially consider particles with a scattering response modelled with a Lorentzian dispersion profile in their individual dipolar and quadrupolar multipolar terms. Then, to offer a structural implementation for such particles, we design core-multishell and disk-multiring particles from realistic materials to satisfy the required conditions for the construction of metasurfaces with full-phase-shift coverage. With these implementations at hand, and as an application, we study the effect of a full-phase-shift coverage on the image quality of a metasurface hologram. The discussion and results are covered in the Supplementary information.

The main purpose of this work is to demonstrate that additional degrees of freedom in the design of Huygens' metasurfaces can be unlocked when considering particles with a more complicated scattering response as their constituents. The particles we propose are exemplary, and many more particles can be considered, driven from the analytical insights. Only recently, the opportunities in exploiting the entire multipolar response of individual particles have been appreciated to tailor their scattering response [18–25]. And with this work, we extend such considerations to Huygens' metasurfaces thereof.

2 Lorentzian particles

The polarisation of particles by an electromagnetic excitation can be quantified by the multipolar polarisability in a Cartesian basis [26, 27]. The particles considered in this article are initially isotropic, and hence, the polarisabilities are scalar. Later, we also present a design for a nonisotropic particle, but this does not change the argumentation. We approximate the response of the particles by their electric and magnetic dipolar and/or quadrupolar polarisabilities. For the initial numerical analysis, we have used a Lorentzian dispersion model for the resonances of the polarisabilities that are corrected for the radiation losses to satisfy the optical theorem [28–32]. In such model, we can easily assume that the electric and magnetic response is equal. The dispersion models used for the dipolar α_d and quadrupolar α_q polarisabilities are defined as follows:

$$\frac{1}{\alpha_d(\omega)} = \frac{\omega_{0d}^2 - \omega^2}{\alpha_{0d}} - \frac{\mathrm{i}\omega}{\alpha_{0d}}\gamma_{\Omega d} - \frac{\mathrm{i}k^3}{6\pi}, \tag{1}$$

$$\frac{1}{\alpha_q(\omega)} = \frac{\omega_{0q}^2 - \omega^2}{\alpha_{0q}/k^2} - \frac{\mathrm{i}\omega}{\alpha_{0q}/k^2}\gamma_{\Omega q} - \frac{\mathrm{i}k^5}{120\pi}, \tag{2}$$

where $k = 2\pi/\lambda$ is the wavenumber in free space, α_{0d} and α_{0q} are related to the oscillator strength, ω_{0d} and ω_{0q} are the resonance frequencies, and $\gamma_{\Omega d}$ and $\gamma_{\Omega d}$ are the Ohmic losses of the dipole and quadrupole resonances, respectively. Considering only nonabsorbing particles, the Ohmic losses throughout the article are always set to zero, i.e. $\gamma_{\Omega d} = \gamma_{\Omega q} = 0$. The electromagnetic duality symmetry of these particles is easily enforced by choosing the free parameters in the electric and magnetic polarisabilities to be the same. Properties

Bereitgestellt von | Karlsruher Institut für Technologie KIT-Bibliothek
Angemeldet
Heruntergeladen am | 27.01.20 13:02

between dipolar and quadrupolar terms, e.g. resonance frequency or oscillator strength, can be distinct, though.

To describe the light scattering from particles with such polarisabilities and to study reflection and transmission through arrays thereof, we rely on a scattering theory that explicitly considers these polarisabilities when defining the T-matrix linked to the scatterer. In the multipole expansion method [26, 33], the T-matrix relates the multipolar scattering coefficients to the incident ones. The T-matrix describes the electromagnetic properties of particles [34, 35]. For an isotropic particle, the corresponding T-matrix in electric/magnetic basis is diagonal, and the elements are the Mie coefficients a_n and b_n [32, 36]. Here, a_n and b_n are multipolar electric and magnetic Mie coefficients, with n denoting the multipole order. A particle having equal electric and magnetic response is said to have electromagnetic duality symmetry, and the particle is called a dual particle [37, 38]. For the isotropic particles considered here, a particle is dual if and only if $a_n = b_n$ for $n = 1, 2, \ldots$. A dual particle preserves the helicity of the impinging light in scattering, i.e. it does not mix the right and left polarisation of the incident light.

The Mie coefficients can be related to the polarisabilities by the following equations [39]:

$$a_1(\omega) = b_1(\omega) = \frac{k^3}{6\pi \mathrm{i}} \alpha_d(\omega), \tag{3}$$

$$a_2(\omega) = b_2(\omega) = \frac{k^5}{120\pi \mathrm{i}} \alpha_q(\omega). \tag{4}$$

Alternatively, the nth order electric a_n and magnetic b_n Mie coefficient for nonabsorbing particles can be modelled according to [31, 32]:

$$a_n(\omega) = \cos\bar{\alpha}_n(\omega) \exp \mathrm{i}\bar{\alpha}_n(\omega), \tag{5}$$

$$b_n(\omega) = \cos\bar{\beta}_n(\omega) \exp \mathrm{i}\bar{\beta}_n(\omega), \tag{6}$$

where we call $\bar{\alpha}_n$ and $\bar{\beta}_n$ the electric and magnetic Mie angles, respectively. Such a model has the least number of degrees of freedom, i.e. only the Mie angles, while it still offers all the characteristic features. This model is particularly useful when systematically driving the properties of the particles through their resonance because only the angle needs to be tuned. For nonabsorbing particles as considered here, $\bar{\alpha}_n$, $\bar{\beta}_n$ are real angles covering a range from $-\pi/2$ to $\pi/2$. An angle equal to zero corresponds to the resonance of the Mie coefficient. Negative/positive angles correspond to the red/blue side of the spectrum of the resonance, respectively.

3 Dipolar and quadrupolar Huygens' metasurfaces

Relying on a T-matrix method formalism for multipolar analysis [32, 34], we have employed a tool for periodically arranged scatterers to study the transmission through two-dimensional lattices of particles. It is an exact approach to calculate reflection and transmission from arrays of identical particles that are characterised by their T-matrix. The latter is being renormalised due to the interaction in the array that we correctly consider in the Ewald summation. We use for our purpose an in-house code, but a description of a program with a relatively similar approach can be found in [40].

To explore the transmission through a periodic arrangement of identical meta-atoms, we use the Lorentzian models in (1) and (2) for the polarisabilities. The corresponding Mie coefficients are shown in amplitude and phase in Figure 1A. While tuning through the resonance, the phase in each coefficient changes up to π. When we arrange such identical particles, characterised by a resonant dipolar or quadrupolar polarisability in either the electric or magnetic multipole moment, in a periodic array and sweeping the illumination wavelength through the resonance, an overall π phase-shift coverage in the spectrum of the transmission is seen (not shown here). Directly in resonance, the transmittance goes to zero. In the complex plane (i.e. real and imaginary transmission), this response corresponds to a circle with a radius of 0.5 and a centre of $0.5 + 0\mathrm{i}$, which touches the origin $0 + 0\mathrm{i}$ at resonance.

However, things change drastically when the condition of duality is met. For a dipolar particle, i.e. a particle characterised by only dipolar polarisabilities, and if the electric and magnetic polarisabilities are equal (i.e. dual), an overall 2π phase-shift coverage in the transmission spectrum t_d is observed (Figure 1B, C), while, as discussed earlier, the transmittance stays unity. In the complex plane, this corresponds to a circle of radius 1 with a centre in origin $0 + 0\mathrm{i}$ (Figure 1B, the red curve) [32]. This response corresponds to a full control over the phase shift.

One step further, and to include higher-order multipoles, if a periodic arrangement of dual dipolar-quadrupole particles is assumed, i.e. particles with $a_1 = b_1 = a_d$, $a_2 = b_2 = a_q$, the complex transmission t_{d+q} as a

Bereitgestellt von | Karlsruher Institut für Technologie KIT-Bibliothek
Angemeldet
Heruntergeladen am | 27.01.20 13:02

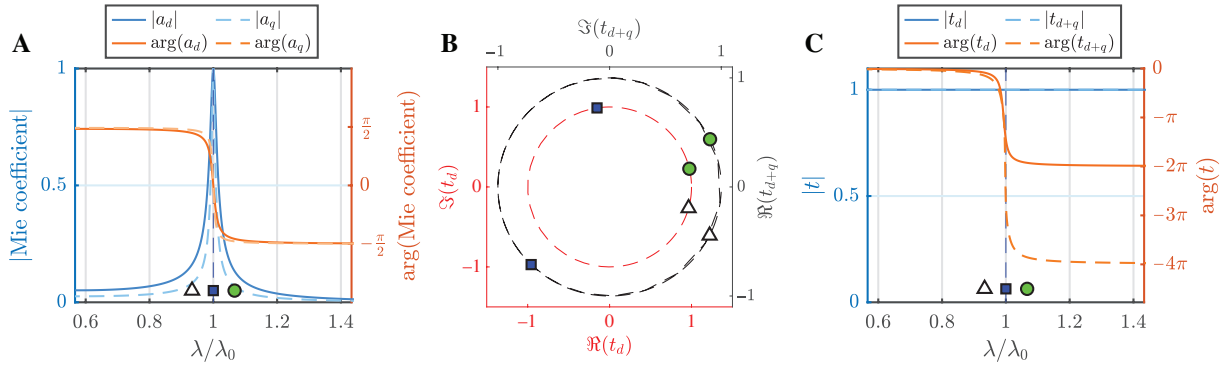

Figure 1: Metasurface transmission in frequency sweep.
(A) The Mie coefficients corresponding to the electric and magnetic dipole and quadrupole resonances. The vertical dark blue dashed line in (A) and (C) shows the resonance wavelength $\lambda_0 = 1500$ nm. (B) The zero-order complex transmission t and (C) its phase $\arg(t)$ and amplitude $|t|$ through a square-array periodic subwavelength arrangement of dual dipole (t_d: red dashed line) and dual dipole-quadrupole (t_{d+q}: black dashed line) Lorentzian particles as function of wavelength. The periodicity is 800 nm. For t_d: $a_1 = b_1 = a_d$, $a_2 = b_2 = 0$ and for t_{d+q}: $a_1 = b_1 = a_d$, $a_2 = b_2 = a_q$. The coloured markers correspond to specific wavelengths as can be seen from (C). The parameters for the Lorentzian model are $\lambda_{0d} = \lambda_{0q} = 1500$ nm, $\alpha_{0q} = 10\alpha_{0d} = 8 \times 10^{10}$ m^3/s^2. The simulations are done in free space.

function of the wavelength will be a double winding circle around the origin 0 + 0i, covering an overall 4π phase shift through the four resonances (Figure 1B, C).

However, any device that is geared toward the modulation of the wavefront is operated at a fixed frequency. There, the phase angle of the transmission is tuned by sweeping the lattice constant of the arrangement. Tuning the lattice constant renormalises the polarisabilities, making the lattice constant a parameter to tune the phase shift of the transmission [39, 41]. For dual dipolar particles, fixed to operate at the resonance wavelength of the polarisabilities, it turns out that a full 2π phase coverage is not possible while tuning the lattice constant. This is shown in Figure 2 when plotting t_d. Eventually, only a range of about $\frac{3}{2}\pi$ is covered (i.e. 75%). This argument is generally valid and independent of the structural implementation of the particle, as the analysis at this stage is done using a generic model for the polarisability of the particles.

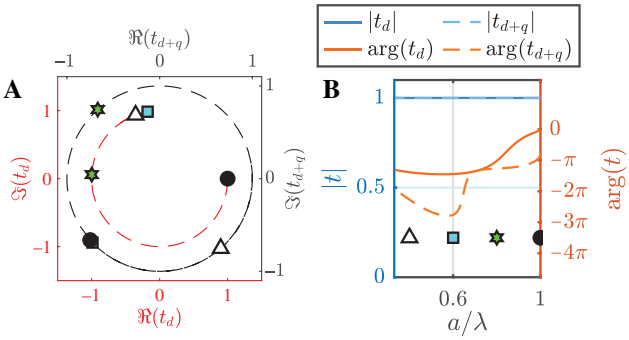

Figure 2: Metasurface transmission in periodicity sweep.
(A) The zero-order complex transmission t and (B) its phase and amplitude through a square-array periodic subwavelength arrangement of dual dipole d and dual dipole-quadrupole $d+q$ Lorentzian particles (Figure 1A) at their individual resonance wavelengths $\lambda_0 = 1500$ nm as a function of the normalised lattice constant. The coloured markers correspond to a specific normalised lattice constant as can be seen from (B).

To mitigate such limitations, we suggest that exploiting quadrupolar resonances in the scatterers along with the dipolar resonances helps to cover the whole phase-shift range of 2π by tuning the periodicity. The larger phase space that could be covered when tuning through the wavelength was a strong indication that this is feasible. Indeed, for a selected example of a square array of particles, a phase coverage slightly larger than 2π can be seen in Figure 2, where t_{d+q} is shown. Again, the particles are operated at the resonance wavelength, which is equal for the dipolar and the quadrupolar terms, and we only tune the lattice constant.

To obtain a more systematic insight into the accessible phase coverage when combining particles with different dipolar and quadrupolar dual resonances and not only those where the operational wavelength is fixed to the resonance wavelength, we resort to the generic model for the Mie coefficients presented in (5) and (6). In particular, we can change there the electric and magnetic Mie angles, $\overline{\alpha}_n$ and $\overline{\beta}_n$, and can study the accessible range for the phase angle in transmission when changing the lattice constant. Selected examples for the phase are shown in Figure 3. Note that as all combinations considered are dual, the transmittance is always unity and for simplicity not shown. In Figure 3A, only dual dipolar particles are considered, while in Figure 3B, dual dipolar-quadrupolar

Bereitgestellt von | Karlsruher Institut für Technologie KIT-Bibliothek
Angemeldet
Heruntergeladen am | 27.01.20 13:02

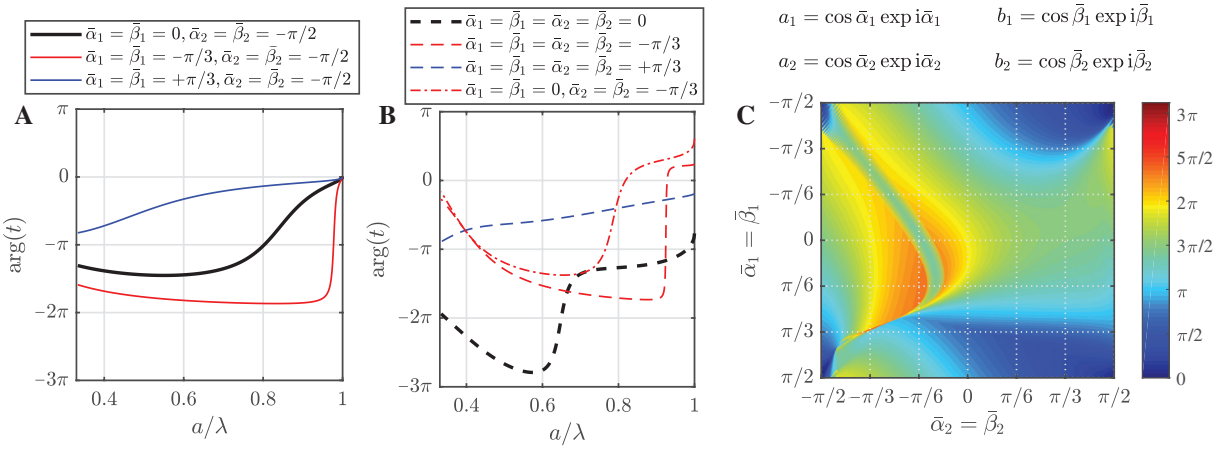

Figure 3: Metasurface phase coverage and the Mie coefficients.
(A) The phase shift achieved by different combinations of dual Mie coefficient angles for dipolar and (B) dipolar-quadrupolar particles as the metasurface constituents as a function of the normalised lattice constant $a/\lambda \in [1/3, 1]$. (C) The phase-shift coverage achieved by all combinations of dual Mie coefficient angles for dipolar-quadrupolar particles. The maximum phase coverage is a sharp strip around $\alpha_1 = \beta_1 = -\alpha_2 = -\beta_2 = 50°$. The simulations are done in free space at a wavelength of 1500 nm, but the results are dependant only on a/λ and is valid for any wavelength.

particles are examined. The larger phase space that is accessible for the dipolar-quadrupolar particles is evident. In Figure 3C, the phase-shift coverage for all dual combinations is shown. The phase-shift coverage corresponds here to the difference in maximum and minimum phase value of the transmission when changing the lattice constant between 1/3 of the operational wavelength and the operational wavelength. In this figure, the slope of the phase dispersion is not shown, and it should be noted that the slope can be very steep at certain points. It remains to mention that this is not always a disadvantage, but this can be beneficially used in optical sensing devices. However, from this figure, we can safely extract a parameter range that covers a range up to around 3π for the phase angle in transmission when tuning through the lattice constant. We can pick any of the related points in this space that offer this functionality and can build a metasurface from such particles. We only need to find a particle that is characterised by the respective Mie coefficient.

4 Multilayered metasurfaces

In this section, we design and propose actual particles that offer the required Mie coefficients necessary to verify the results derived for Lorentzian particles. We show that by sweeping the lattice constant within the physical constraints, i.e. the lattice constant has to be smaller than the wavelength to preserve the nondiffracting nature of the metasurface, a metasurface made out of identical dipolar particles cannot give us a full-phase-shift coverage in the transmission and unity transmittance. However, we show that using identical designed dipolar-quadrupolar particles, the aforementioned requirement can be satisfied.

First, we design a dipolar core-multishell particle, abbreviated in the following as c_1, to meet dual dipole resonance at $\lambda = 1500$ nm, i.e. $a_1 = b_1 = 1$ and $a_{n>1} \approx b_{n>1} \approx 0$. For the design of the core-multishell particles, we have used a particle swarm optimisation method [31, 42, 43]. We consider a core-multishell particle with up to two shells. The core and the shells were allowed to be made from isotropic nonmagnetic materials with a refractive index in the range from 1 to 7. For the optimised particle, the Mie coefficients as a function of the wavelength are shown in Figure 4A. Clearly, at the desired operational wavelength of $\lambda = 1500$ nm, the dipolar coefficients are at unity, while higher-order Mie coefficients are negligible. The transmission through the metasurface made from such particles at the resonance wavelength $\lambda = 1500$ nm as a function of the normalised lattice constant is shown in Figure 4C and D (t_{c_1}). As expected, the results are very similar to t_d in Figure 2; the phase coverage is about 75% of the full 2π, and as can be seen, it is not possible to have the full-phase coverage within the possible lattice constants. Note that the lattice constant is bound by the physical size of the actual particle ($a = 2 \times 346.65 = 693.30$ nm) at the lower end and by the diffraction limit ($a = \lambda = 1500$ nm) on the upper end.

Next, we want to design a core-multishell particle that can provide the full-phase coverage of the transmission

Bereitgestellt von | Karlsruher Institut für Technologie KIT-Bibliothek
Angemeldet
Heruntergeladen am | 27.01.20 13:02

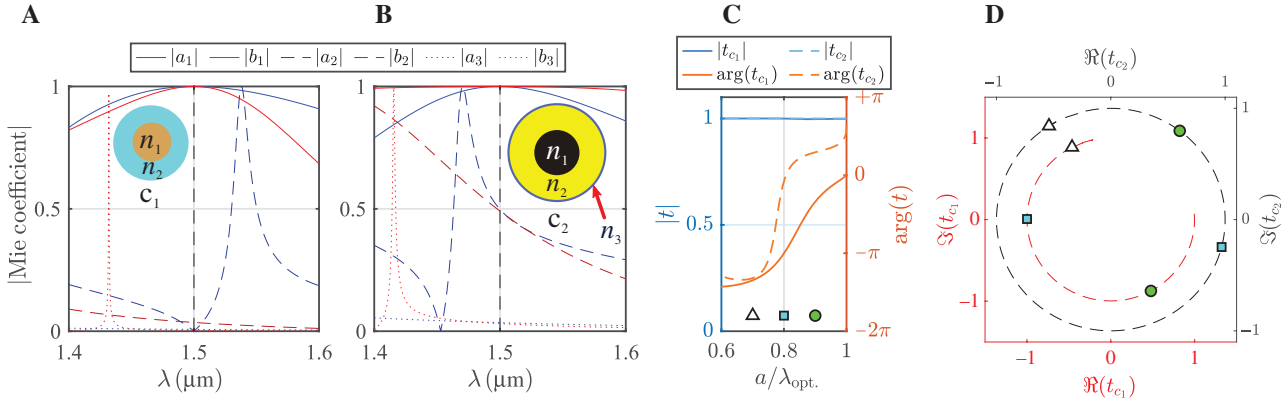

Figure 4: Transmission of core-multishell metasurfaces.
(A) Mie coefficients of the dipolar c_1 (inset picture) and (B) dipolar-quadrupolar c_2 (inset picture) core-multishell particles. The vertical black dashed line is the design operating wavelength $\lambda_{opt.}=1500$ nm. (C) Phase and amplitude and (D) the complex zero-order transmission of a square array of c_1 and c_2 particles. For core-multishell particles (c_1), the design parameters are $[r_1, r_2, n_1, n_2]=[181.35\text{ nm}, 346.65\text{ nm}, 7, 2.5]$, and the derived Mie coefficient angles at $\lambda_{opt.}=1500$ nm are $\bar{\alpha}_1=\bar{\beta}_1=0$, $\bar{\alpha}_{n>1}\approx\bar{\beta}_{n>1}=-\pi/2$. For core-multishell particles (c_2), the design parameters are: $[r_1, r_2, r_3, n_1, n_2, n_3]=[213.30\text{ nm}, 447.75\text{ nm}, 458.55\text{ nm}, 5.96, 1.57, 4.96]$, and the derived Mie coefficient angles at $\lambda=1500$ nm are $\bar{\alpha}_1=\bar{\beta}_1=0$, $\bar{\alpha}_2=\bar{\beta}_2=-\pi/3$, $\bar{\alpha}_{n>2}\approx\bar{\beta}_{n>2}=-\pi/2$. The simulations are done in free space but can be scaled for any embedding and wavelength.

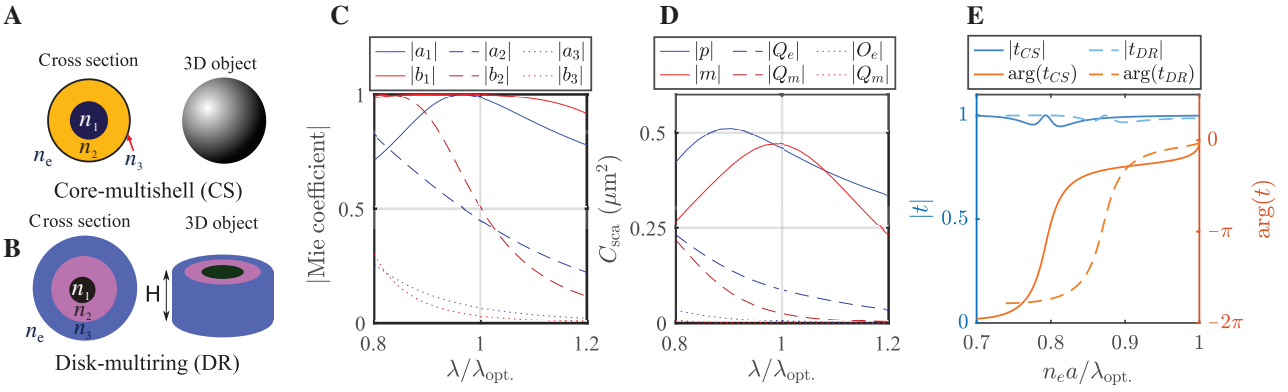

Figure 5: Transmission of designed dual-quadrupole metasurfaces.
(A) Designed core-multishell (CS) and (B) disk-multiring (DR) particles at a design wavelength of $\lambda_{opt.}=1500$ nm: The parameters derived from particle swarm optimisation for the core-multishell particle: $[n_1, n_2, n_3]=[3.67, 2.16, 4]$ and $[r_1, r_2, r_3]=[135, 354, 365]$ nm, where $n_e=1.44$ is the refractive index of the embedding medium. The parameters derived from particle swarm optimisation for the disk-multiring particle: $[n_1, n_2, n_3]=[1.9, 3.34, 2.2]$ and $[r_1, r_2, r_3, H]=[157.9, 284.8, 375, 361.2]$ nm, where $n_e=1.44$ is the refractive index of the embedding medium. (C) The corresponding Mie coefficients and (D) multipolar scattering cross-section contribution of the core-multishell and the disk-multiring particle, respectively. (E) The zero-order phase angle and amplitude of transmission through a square array arrangement of the core-multishell (t_{CS}) and disk-multiring (t_{DR}) particle embedded in a homogeneous environment $n_e=1.44$ as a function of the normalised lattice constant.

phase angle in the metasurface with lattice constant tuning. As we showed in the previous section, a suitable particle would require both dipolar and quadrupolar responses. An extra requirement, here for a hologram as a direct application, is that the phase-shift change as a function of the lattice constant is smooth and not steep. This is experimentally important to be able to use the full potential of the lattice sweep.

Based on our simulations, to achieve full-phase-shift coverage and a smooth phase-shift variation, a particle with the designed Mie coefficient angle of $\bar{\alpha}_1=\bar{\beta}_1=0$, $\bar{\alpha}_2=\bar{\beta}_2=-\pi/3$, $\bar{\alpha}_{n>2}\approx\bar{\beta}_{n>2}\approx-\pi/2$ is deemed suitable. The dispersion of the phase shift is already shown in Figure 3B (the red dash-dotted line).

Then, based on the required parameters, using the particle swarm optimisation, we have designed a core-multishell particle to fulfil $\bar{\alpha}_1=\bar{\beta}_1=0$, $\bar{\alpha}_2=\bar{\beta}_2=-\pi/3$, $\bar{\alpha}_{n>2}\approx\bar{\beta}_{n>2}\approx-\pi/2$ at a wavelength of 1500 nm. The refractive index of the shells is bound between 1 and 6. At this stage, the large refractive index has been chosen to clearly

Bereitgestellt von | Karlsruher Institut für Technologie KIT-Bibliothek
Angemeldet
Heruntergeladen am | 27.01.20 13:02

demonstrate the feasibility. Further below, the design of particles is presented that are made from materials with properties offered by naturally available materials in near infrared (NIR). The designed particle in Figure 4B is abbreviated in the following as c_2. The Mie coefficients and the lattice constant sweep of the transmission are shown in Figure 4B–D (t_{c_2}). The result verifies our initial expectation that with dipolar-quadrupolar particles a full 2π phase-shift coverage is achievable. The simulations are done in free space. In a homogeneous environment with refractive index n_e, the results remain the same if the particle radii and the corresponding refractive indexes are down-scaled and up-scaled by a factor of n_e, respectively.

Although nonabsorbing natural materials with a refractive index of up to 7 can be found at frequencies up to the mid-infrared spectrum [44], at NIR, we are limited to a maximum refractive index of 4 offered by natural materials. In this refined analysis, we would like to propose structures that can be used to realise Huygens' dipole-quadrupole metasurfaces at NIR frequencies. Therefore, we have limited the refractive index to a range of 1 to 4 in the optimisation procedure in the following. We continue to assume a design wavelength of 1500 nm, and we have used again the particle swarm optimisation. We designed two different structures. First was a core-multishell particle considering these more realistic material properties. Second, we designed a disk-multiring particle that can indeed be realised with top-down nanostructure technology. In both cases, we considered a homogeneous dielectric environment as the embedding medium (Figure 5A, B). The electromagnetic properties of the individual optimised structures are shown in Figure 5C and D. The calculations of the optical response from the disk-multiring structure are done with JCMwave, a finite element solver for Maxwell's equations. Although the particles are not perfectly dual, they have a strong quadrupole component. The results for the transmission through an arrangement of such particles are shown in Figure 5E. The results show promising results. The core-multishell and disk-multiring metasurface covers 97% and 90% of the total phase coverage, while their transmittance keeps near unity.

5 Conclusion

We have shown that with identical dipolar particles achieving the full-phase shift with lattice constant tuning is practically not possible in Huygens' metasurfaces. However, using optimised dipolar-quadrupolar particles, metasurfaces can be designed to cover the full 2π phase shift. We have designed core-multishell and disk-multiring particles to support our results. Holograms made from such dipolar-quadrupolar particles show an improved performance, as documented in the Supplementary information.

Acknowledgement: This research has been funded by the Deutsche Forschungsgemeinschaft (DFG, German Research Foundation) under Germany's Excellence Strategy via the Excellence Cluster 3D Matter Made to Order (EXC-2082/1–390761711) and under the priority program SPP 1839 Tailored Disorder (RO 3640/7-2 and STA 1426/1-2 under project no. 278747906). A.R. also acknowledges support from the Karlsruhe School of Optics and Photonics (KSOP). R.A. acknowledges financial support provided by the Alexander von Humboldt Foundation. The authors are grateful to the company JCMwave for their free provision of the FEM Maxwell solver JCMsuite with which the simulations on the disk-multiring structures in this work have been performed. They acknowledge support by the DFG and Open Access Publishing Fund of Karlsruhe Institute of Technology.

References

[1] Fernandez-Corbaton I. Forward and backward helicity scattering coefficients for systems with discrete rotational symmetry. Opt Express 2013;21:29885.
[2] Pfeiffer C, Grbic A. Metamaterial Huygens' surfaces: tailoring wave fronts with reflectionless sheets. Phys Rev Lett 2013;110:197401.
[3] Staude I, Schilling J. Metamaterial-inspired silicon nanophotonics. Nat Photonics 2017;11:274–84.
[4] Decker M, Staude I, Falkner M, et al. High-efficiency dielectric Huygens' surfaces. Adv Opt Mater 2015;3:813–20.
[5] Kuznetsov AI, Miroshnichenko AE, Brongersma ML, Kivshar YS, Luk'yanchuk B. Optically resonant dielectric nanostructures. Science 2016;354:aag2472.
[6] Kamali SM, Arbabia E, Arbabi A, Faraon A. A review of dielectric optical metasurfaces for wavefront control. Nanophotonics 2018;7:1041–68.
[7] Chen M, Kim M, Wong AMH, Eleftheriades GV. Huygens' metasurfaces from microwaves to optics: a review. Nanophotonics 2018;7:1207–31.
[8] Liu S, Vaskin A, Campione S, et al. Huygens' metasurfaces enabled by magnetic dipole resonance tuning in split dielectric nanoresonators. Nano Lett 2017;17:4297–303.
[9] Chong KE, Staude I, James A, et al. Polarization-independent silicon metadevices for efficient optical wavefront control. Nano Lett 2015;15:5369–74.
[10] Yu YF, Zhu AY, Paniagua-Domínguez R, Fu YH, Luk'yanchuk B, Kuznetsov AI. High-transmission dielectric metasurface with 2π phase control at visible wavelengths. Laser Photonics Rev 2015;9:412–8.
[11] Staude I, Miroshnichenko AE, Decker M, et al. Tailoring directional scattering through magnetic and electric resonances in subwavelength silicon nanodisks. ACS Nano 2013;7:7824–32.

Bereitgestellt von | Karlsruher Institut für Technologie KIT-Bibliothek
Angemeldet
Heruntergeladen am | 27.01.20 13:02

[12] Chen X, Huygens' YP. Metasurface made of core-shell spherical nanoparticles. metamaterials, metadevices, and metasystems. Int Soc Opt Photonics 2018;10719:1071907.
[13] Khorasaninejad K, Chen WT, Devlin RC, Oh J, Zhu AY, Capasso F. Metalenses at visible wavelengths: diffraction-limited focusing and subwavelength resolution imaging. Science 2016;352:1190–4.
[14] Jin C, Afsharnia M, Berlich R, et al. Dielectric metasurfaces for distance measurements and three-dimensional imaging. Adv Photonics 2019;1:036001.
[15] Wang L, Kruk S, Tang H, et al. Grayscale transparent metasurface holograms. Optica 2016;3:1504–5.
[16] Shalaev MI, Sun J, Tsukernik A, Pandey A, Nikolskiy K, Litchinitser NM. High-efficiency all-dielectric metasurfaces for ultracompact beam manipulation in transmission mode. Nano Lett 2015;15:6261–6.
[17] Ollanik AJ, Smith JA, Belue MJ, Escarra MD. High-efficiency all-dielectric Huygens metasurfaces from the ultraviolet to the infrared. ACS Photonics 2018;5:1351–8.
[18] Liu W, Kivshar YS. Generalized Kerker effects in nanophotonics and meta-optics [invited]. Opt Express 2018;26:13085–105.
[19] Kruk S, Hopkins B, Kravchenko II, Miroshnichenko A, Neshev DN, Kivshar YS. Invited article: broadband highly efficient dielectric metadevices for polarization control. Apl Photonics 2016;1:030801.
[20] Shamkhi HK, Baryshnikova KV, Sayanskiy A, et al. Transverse scattering and generalized Kerker effects in all-dielectric Mie-resonant metaoptics. Phys Rev Lett 2019;122:193905.
[21] Terekhov PD, Babicheva VE, Baryshnikova KV, et al. Multipole analysis of dielectric metasurfaces composed of nonspherical nanoparticles and lattice invisibility effect. Phys Rev B 2019;99:045424.
[22] Babicheva VE, Evlyukhin AB. Analytical model of resonant electromagnetic dipole-quadrupole coupling in nanoparticle arrays. Phys Rev B 2019;99:195444.
[23] Alaee R, Rockstuhl C, Fernandez-Corbaton I. Exact multipolar decompositions with applications in nanophotonics. Adv Opt Mater 2019;7:1800783.
[24] Chen J, Ng J, Lin Z, et al. Optical pulling force. Nat Photonics 2011;5:531–34.
[25] Mobini E, Rahimzadegan A, Rockstuhl C, et al. Theory of optical forces on small particles by multiple plane waves. J Appl Phys 2018;124:173102.
[26] Bohren CF, Huffman DR. Absorption and scattering of light by small particles. New York, NY, USA, John Wiley & Sons, 2008.
[27] Tretyakov S. Analytical modeling in applied electromagnetics. Norwood, MA, USA, Artech House, 2003.
[28] Sipe JE, Kranendonk JV. Macroscopic electromagnetic theory of resonant dielectrics. Phys Rev A 1974;9:1806–22.
[29] Novotny L, Hecht B. Principles of nano-optics. Cambridge, England, UK, Cambridge University Press, 2012.
[30] Bonin KD, Kresin VV. Electric-dipole polarizabilities of atoms, molecules, and clusters. Singapore, World Scientific, 1997.
[31] Rahimzadegan A, Alaee R, Fernandez-Corbaton I, et al. Fundamental limits of optical force and torque. Phys Rev B 2017;95:035106.
[32] Rahimzadegan A, Arslan D, Suryadharma RNS, et al. Disorder-induced phase transitions in the transmission of dielectric metasurfaces. Phys Rev Lett 2019;122:015702.
[33] Jackson JD. Classical electrodynamics. New York, NY, USA, Wiley, 1999.
[34] Mishchenko MI, Travis LD, Mackowski DW. T-matrix computations of light scattering by nonspherical particles: a review. J Quant Spectrosc Radiat Transf 1996;55:535–75.
[35] Rahimzadegan A, Fruhnert M, Alaee R, et al. Optical force and torque on dipolar dual chiral particles. Phys Rev B 2016;94:125123.
[36] Fruhnert M, Fernandez-Corbaton I, Yannopapas V, et al. Computing the T-matrix of a scattering object with multiple plane wave illuminations. Beilstein J Nanotechnol 2017;8:614–26.
[37] Fernandez-Corbaton I, Zambrana-Puyalto X, Tischler N, et al. Electromagnetic duality symmetry and helicity conservation for the macroscopic maxwell's equations. Phys Rev Lett 2013;111:060401.
[38] Fernandez-Corbaton I. Helicity and duality symmetry in light matter interactions: theory and applications (PhD thesis). Sydney, Australia, Macquarie University, 2014. eprint: arXiv:1407.4432.
[39] Evlyukhin AB, Reinhardt C, Zywietz U, et al. Collective resonances in metal nanoparticle arrays with dipole-quadrupole interactions. Phys Rev B 2012;85:245411.
[40] Stefanou N, Yannopapas V, Modinos A. MULTEM 2: a new version of the program for transmission and band-structure calculations of photonic crystals. Comput Phys Commun 2000;132:189–6.
[41] Babicheva VE, Evlyukhin AB. Metasurfaces with electric quadrupole and magnetic dipole resonant coupling. ACS Photonics 2018;5:2022–33.
[42] Lee KY, El-Sharkawi MA. Modern heuristic optimization techniques: theory and applications to power systems. Vol. 39. New York, NY, USA, John Wiley & Sons, 2008.
[43] Rahimzadegan A, Rockstuhl C, Fernandez-Corbaton I. Core-shell particles as building blocks for systems with high duality symmetry. Phys Rev Appl 2018;9:054051.
[44] Baranov DG, Zuev DA, Lepeshov SI, et al. All-dielectric nanophotonics: the quest for better materials and fabrication techniques. Optica 2017;4:814–25.

Supplementary Material: The online version of this article offers supplementary material (https://doi.org/10.1515/nanoph-2019-0239).

Bereitgestellt von | Karlsruher Institut für Technologie KIT-Bibliothek
Angemeldet
Heruntergeladen am | 27.01.20 13:02